ELSEVIER

Journal of Chromatography A, 811 (1998) 181–192

JOURNAL OF CHROMATOGRAPHY A

Experimental factors in pulsed electrochemical detection in capillary electrophoresis

Jenny Wen, Richard M. Cassidy*, Andrzej S. Baranski

Chemistry Department, University of Saskatchewan, 110 Science Place, Saskatoon, SK S7N 5C9, Canada

Received 12 November 1997; received in revised form 26 March 1998; accepted 6 April 1998

Abstract

A number of experimental approaches that should offer improved S/N in electrochemical detection were evaluated and compared. In addition, to evaluate and optimize the electrochemical response behavior of analytes under actual CE conditions, an on-line cyclic voltammetry (CV) system was developed. The experimental parameters examined included waveform shape, waveform frequency and various signal treatments, using a lock-in amplifier and Fourier analysis. A multiple-step pulse waveform provided the maximum S/N enhancement [up to 10-fold relative to pulse amperometric detection (PAD)], with detection limits in the range of $2\cdot10^{-8}$ to $2\cdot10^{-7}$ mol/l. The use of the second harmonic from Fourier analysis offered the best improvement in baseline stability. Other approaches such as high pulse frequency (100 to 200 Hz), data collection over selected time windows, digital filters and average smoothing also enhanced S/N 2- to 5-fold relative to PAD. On-line CV studies showed that the adsorption of organic electrolytes on electrode surfaces can inhibit O_2 reactions, and thus give low and stable background currents without O_2 removal. The CV studies also showed that detection of Pb^{2+}, Cu^{2+} and Ag^{+} affected subsequent electrode response, and that H^{+} evolution contributed to the cathodic signals of the analytes Ni^{2+}, Co^{2+} and Zn^{2+}.

Keywords: Electrochemical detection; Detection, electrophoresis; Cyclic voltammetry; Metal cations

1. Introduction

Electrochemical detection is attractive for capillary electrophoresis (CE) because μm-electrodes can provide small ohmic distortion in detection systems, high sensitivities for small inner diameter (I.D.) capillaries and rapid response when concentration or potential is changed at the electrode. The fast response of μm-electrodes is particularly important for the application of high-frequency potential waveforms. Most electrochemical detection is based on amperometric detection principles. Of the various amperometric approaches, constant-voltage detection is the simplest. Direct reductive and oxidation methods with constant-voltage works well for the determination of some analytes, such as catechols [1] and chlorophenol [2] however, inconsistent response is often observed due to electrode fouling from sample matrixes and/or analyte reaction products [3,4]. One possible approach to prevent fouling of the electrode surface is to apply pulsed potentials. Pulsed amperometric detection (PAD) uses a multi-step potential waveform to detect analytes and to clean and reactivate the electrode surface. Since PAD was introduced to liquid chromatography (LC) [5,6] it has been shown to improve the long-term stability

*Corresponding author.

0021-9673/98/$19.00
PII: S0021-9673(98)00283-0

of electrode response for amino acids [7,8], carbohydrates [9,10] and sulfur-containing compounds [11,12]. In previous studies [13] we found that PAD of metal ions was reproducible ($\leq$5% over 14 h) with detection limits in the range of 10^{-5} to 10^{-7} mol/l; these detection limits are similar to those reported for the PAD of other electroactive compounds in LC and CE [14–16]. Although these detection limits are sufficient for many samples, there are instances where lower detection limits are required. Thus, it would be desirable if other more sensitive electrochemical detection approaches could be developed.

Possible parameters in PAD that may offer improved signal-to-noise ratio (S/N) include waveform shape, waveform frequency and signal analysis. Previous pulsed amperometric studies in LC and CE have used a simple 2- or 3-step potential waveforms [17–19], and frequencies of 1 to 8 Hz [19–21]. Higher frequencies should offer larger currents, and different sensitivity for kinetically controlled processes (which under certain conditions can improve the selectivity of detection). In addition, if the applied waveform contains sections where the potential is cycled very rapidly, it may be possible to momentarily trap analytes at the electrode to permit current measurements over several adsorption/desorption steps. An additional approach that may improve S/N is to make use of current–voltage characteristics that exist on the application of pulsed voltages to an electrode. The analysis of current vectors based on amplitude and phase-angle relationships can help differentiate between faradaic and capacitance currents [22]; this approach may reduce the capacitance current component which is an important part of background noise. Another approach for S/N enhancement is to utilize the different distributions of signal and noise in fundamental and higher harmonic components. This approach can be achieved via both digital Fourier analysis and lock-in amplifiers. Recently, studies with a flow injection system have shown that 2nd harmonics obtained from application of sinusoidal waveform may offer some advantages for detection of carbohydrates at a Cu electrode [23]. All of these approaches offer possible advantages, and it would be useful to have a systematic study and comparison of them.

In our previous PAD studies [13] certain experimental conditions for some metal ions caused poor response, deformed peaks, baseline-shifted peaks, and even negative peaks. These problems appeared to be related to slow kinetics and/or the changes in the electrode surface as a result of interaction with the analytes or electrolytes. Since these problems are important for the optimization of PAD in CE, there is a need to understand the electrochemical behavior of analytes and co-existing species at these electrodes. A possible approach that may help is on-line CE–cyclic voltammetry (CV). CV is commonly used to study the thermodynamics and kinetics of electrochemical reactions at electrode–solution interfaces, but with conventional CV it is difficult to differentiate small analyte signals from fluctuating background currents. Single-scan voltammetry has been used for open-tubular LC [24], and multiple-step voltammetry has been used in CE [25,26]. In a recent paper [26] it has been shown that voltammetric detection with a fiber electrode inserted into a decoupled capillary presents serious resistance problems for scanning. The use of an end-capillary disk electrode should reduce these problems and permit much faster scanning, and permit application of CV waveforms.

The two main goals of the present study were: firstly, develop on-line fast-scanning CV to examine the electrochemical behavior of analytes and electrolytes at low concentration levels used in CE; and secondly, evaluate different experimental approaches for improvement of S/N in electrochemical CE detection. The parameters studied included waveform shape, waveform frequency and data treatment, such as vector and harmonic analysis. The test analytes chosen for this study were a series of metal ions. These were selected because they show a wide range of electrochemical behavior, and thus the results should be representative of a number of other electroactive species.

2. Experimental

2.1. CE apparatus and procedures

Separation capillaries were 25 μm I.D.×350 μm O.D. (fused-silica, Polymicro Technology, Phoenix, AZ, USA) and were washed before use with water,

0.1 mol/l HCl and operating electrolytes [13] to obtain reproducible electroosmotic flow (EOF). EOF was monitored via the oxidation signal of catechol (99%, Aldrich, Milwaukee, WI, USA), or via the baseline change after injecting water. For capillary storage, a flow of electrolyte was maintained at ~10 cm height differential. The input of the high-voltage (0 to 30 kV) power supply (Spellman, High Voltage Electronics, Plainview, NY, USA) was placed in a Plexiglas box with an interlock switch on the access door for protection. Analytes were introduced into capillaries via 5 kV electrokinetic or 10 cm hydrodynamic injection for 10 s. Under these sampling conditions, for hydrodynamic injection, the volume introduced into the end of the capillary was calculated [27] to be approximately 1.7 nl; and for electrokinetic injection, the amount of sample injected [27] for Tl^+ was $1.8 \cdot 10^{-13}$ mol which was equal to the analyte in 3.7 nl of the sample solution, and the sample volume injected into capillary by EOF was approximately 0.62 nl.

2.2. Electrochemical system

The three-electrode electrochemical system consisted of a saturated KCl calomel reference electrode (Fisher Scientific, Ottawa, Canada), a Pt wire (0.5 mm^2) counter electrode, and 25 μm Au or Pt disk working electrodes. In these present studies it was found that the analytical performance of the Au electrodes was slightly better than that for Pt electrodes, and consequently Pt electrodes were not used extensively in the quantitative aspects of these studies. The construction and preconditioning of working electrodes has been described previously [13]. The alignment and distance between the electrodes and the end of the separation capillary (~20 μm) was adjusted with a XYZ micropositioner (Klinger, Garden City, NY, USA). The detection cell and potentionstat were placed in a Faraday cage to minimize environmental noise. Details of the construction of the potentionstat has been described elsewhere [28]. The electrochemical system was controlled with a pentium/16 MB RAM IBM personal computer equipped with a PCL-818 data acquisition board (B&C Microsystem, Sunnyvale, CA, USA). The lock-in amplifier was a Model 5301, EG&G Princeton Applied Research, Princeton, NJ, USA, operated with a 0.1 s time constant. Cathodic currents were designated as positive currents and anodic currents as negative currents. For most of the present results, the relative error was ca. 0.01; three to four measurements were made.

Pulses for amperometric detection were either bipolar with a frequency of 5 to 1000 Hz, or consisted of a combination of several square pulses with different frequencies; these more complicated waveforms are discussed in Section 3.2. For most PAD studies with a simple two-step waveform, the analytes were reduced in the first part of the waveform at −1200 to −700 mV, and oxidation of analytes was in the second step at 100 to 200 mV [13]. For PAD with frequencies from 5 to 8 Hz, the analytical signal monitored was the average current measured over the last 24, 48 or 72 ms of the reduction pulse for cathodic analysis, and over the first 48 or 72 ms of the oxidative step for anodic analysis. For PAD with frequencies of more than 7.5 Hz, the signal was selected by four different methods: the average current measured over whole reduction pulse for cathodic analysis; the average current over whole oxidation pulse for anodic analysis; total current (cathodic current minus anodic current); and average cathodic and anodic current over one waveform pulse. These different approaches to data collection were used because the relationships between the factors contributing to S/N as waveform frequencies are increased are complex, and the optimum approach is difficult to predict.

For PAD, and for most CV experiments, oxygen was not removed except as indicated. For the CV studies, the potential waveform had a conventional triangular shape combined with a preconcentration period: ~50 ms at an initial potential (−1200 to −700 mV) and then scanned to a switching potential (−100 to 200 mV). The selection of the CV potential range depended on the standard potentials of analytes. The voltammogram was recorded at ~4000 data points per second (each point was an average of 10–17 A/D conversions). Several voltammograms (≥15) were obtained while a narrow analyte peak passed by the working electrode.

2.3. Reagents

All chemicals were of analytical grade and were

used without further purification. The solutions were prepared from double-distilled deionized water (Corning, Mega-Pure system, MP-6A and D2, Corning, NY, USA), and were stored in the dark. The background electrolyte for separation and detection of the metal ions was 0.030 mol/l creatinine (Sigma, St. Louis, MO, USA) and 0.008 mol/l α-hydroxyisobutyric acid (HIBA) (98%, Aldrich), and the pH value was adjusted with acetic acid (~30 m*M*) to 4.8. The electrolytes were remade every two to three months and were replaced daily in the separation reservoir to avoid chemical and pH changes. Metal ion stock solutions (~ 0.01 mol/l) were diluted to the desired concentration with operating electrolyte prior to use. All CE solutions were filtered through a 0.2-μm nylon-66 membrane syringe filter (Cole-Parmer). Reagent grade metal salts used were: thallium nitrate and nickel nitrate (Fisher Scientific, Fair Lawn, NJ, USA); lead nitrate, (Anachemia, Montreal, Canada); cadmium nitrate and zinc nitrate (Merck, Rahway, NJ, USA); silver acetate (BDH, Toronto, Canada); cobalt acetate (General Chemical Division, Allied Chemical and Dye, NY, USA); and cupric acetate (BDH, Toronto, Canada).

2.4. Signal analysis techniques

The basic principles involved in the special data treatments used in these studies can be found elsewhere [22]. Three of the approaches used involved isolation of non-symmetrical analyte signals from the more symmetrical background signals (e.g., capacitance currents). When analyte reduction or oxidation occurs the relation between current and potential is such that different phase relationships are observed for analyte and background signals. Also, because current–potential relationships are described by an exponential function, non-linear behaviour is obtained, which generates higher harmonics especially when current–time dependencies for the reduction and the oxidation processes are significantly different. Thus one can expect that phase-sensitive detection and/or harmonic analysis might lead to a significant improvement in *S*/*N*. In addition to the above data treatment processes, standard Fourier-transform filters, moving-average smoothing and polynomial smoothing were also examined to improve *S*/*N*.

3. Results and discussion

3.1. On-line cyclic voltammetry

3.1.1. Background CV studies

On-line CV was examined to determine if it could provide useful information about the electrochemical reactions occurring under the CE experimental conditions. Since 25 μm Au and Pt electrodes had provided good analytical response previously [13] these electrodes were chosen for these studies. When the distance between the end of the capillary and the electrode was more than 40 μm, the analytical signal decreased due to dilution, and when it was <20 μm, both background noise and the shift in the working-electrode potential began to increase significantly. Thus the distance was adjusted to $\sim 20 \pm 5$ μm to maximize *S*/*N*, to reduce peak broadening, and to maintain small potential shifts. For a wide range of experimental conditions the shift in electrode potential observed on application of a 20 kV separation voltage was in the range of 100 to 150 mV, but week-to-week reproducibility of CV peak potential was ≤ 50 mV. A scan rate of 20 V/s was used to ensure that electrode behavior could be monitored at several points across a narrow CE peak.

Electrolyte composition can influence the properties of the double layer at the electrode–solution interface, and this may affect electrochemical reactions at the electrode. To evaluate the role of the electrolytes used in this investigation, background cyclic voltammograms were studied at a Au electrode in 8 mmol/l HIBA and 30 mmol/l creatinine. The results in Fig. 1A show that a peak appeared at -180 mV, which is the region expected for O_2 reduction. However, degassing (Ar or N_2) did not eliminate the peak, and caused little change in the voltammogram. It is known [29,30] that some organic compounds adsorb on Au and Pt surfaces, and thus the peak at -180 mV might be from the adsorption of HIBA or creatinine at the electrode. Similar behavior, with slight shifts in shape and position of the adsorption peak, was also observed with succinic acid and creatinine, and with an acetic acid buffer. To help confirm that the peak resulted from the adsorption of organic compounds at the electrode, cyclic voltammograms were recorded in phosphate, perchlorate and nitrate electrolytes (20–

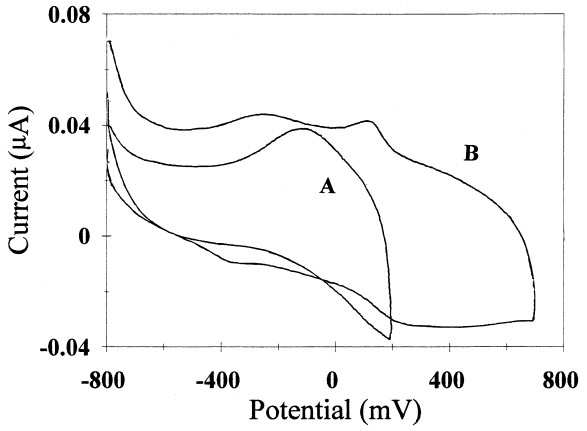

Fig. 1. On-line cyclic voltammograms with 25 μm Au electrode for HIBA–creatinine electrolytes. Experimental conditions: cathodic current is considered as positive current; applied potentials, −800 mV for 55 ms and then scanned to 200 mV (A) or 700 mV (B) at 20 V/s; electrolyte, 0.030 mol/l creatinine and 0.008 mol/l HIBA at pH 4.8; separation voltage, 20 kV over a 60 cm×25 μm capillary.

60 m*M*, pH=3.2~4.7). These electrolytes are expected to exhibit less adsorption on the electrode, and adsorption has been shown to be particularly weak for perchlorate [31]. In all cases a significant amount of the background response observed at negative potentials was easily removed via degassing. The above studies suggest that organic molecules in the electrolytes can decrease background currents, possibly due to their adsorption at the active sites on the electrode, which would alter capacitance currents and/or changes in the O_2 reduction process. This conclusion is also supported by the results reported for acridine and quinoline derivatives [32].

During both PAD and on-line CV studies it was found that the use of high positive potentials during one part of the applied waveform was always accompanied by higher background currents and noise. For example, background noise with a maximum CV potential of 700 mV increased 2–4-times compared to that at 200 mV. A typical result for cyclic voltammograms of background electrolytes obtained at higher positive potentials is shown in Fig. 1B. Compared to Fig. 1A, the capacitance current is slightly larger, and the overall response is changed. When this solution was degassed (N_2 or Ar) the only significant change was the elimination of the peak at 100 mV. While the position of this peak is at too positive a voltage for O_2 reduction, its disappearance upon degassing suggests it is associated with the presence of O_2. These results suggest that the organic adsorption layer may have been reduced or stripped off the electrode at the more positive potential, which would permit O_2 reactions; removal of the adsorbed organics should also reduce the thickness of the double layer which could cause larger capacitance currents. Thus under these conditions, background noise is expected to increase by ~2- to 3-fold. Similar behavior has also been described by Chen et al. [33] who studied the mechanism of metal deposition at Au electrodes in perchlorate solutions. Another factor may be the formation of oxide on the Au surface resulting in pitting (AuOH or AuO) and roughening of the surface, which may lead to a higher noise at potentials of +650 mV to 1300 mV [34].

Background CV studies were also performed at different potentials with Pt electrodes in electrolytes consisting of 8 mmol/l HIBA with 30 mmol/l creatinine, and 10 mmol/l succinic acid with 30 mmol/l creatinine (both at ~pH 4.8). Results similar to those reported above for Au electrodes were obtained. Thus, it appears that organic electrolytes adsorb at Au and Pt electrode surfaces to inhibit capacitance currents and/or O_2 reactions, which leads to smaller background noise and more stable baselines. These studies also suggest that these organic molecules can be desorbed at higher positive potentials, and that for maximum S/N high positive potentials should be avoided.

A typical set of cyclic voltammograms obtained across the CE peak of analyte (with background subtraction) is shown in Fig. 2. Each of the cyclic voltammograms in Fig. 2 was recorded at a different point on a Tl^+ peak (~150 ms intervals). These results show that the on-line CV system gave good CV signals even for concentrations down to ~2 μmol/l. This sensitivity was up to 100-fold improved relative to that obtained with off-line CV analysis. This improvement appears to be related to a stable background signal produced by transfer of the analyte ions from the injected sample solution into the homogeneous background electrolyte.

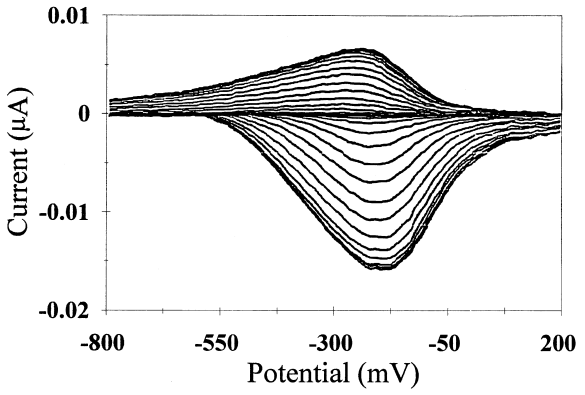

Fig. 2. On-line cyclic voltammograms across Tl^+ peaks with 25 μm Au electrode. Experimental conditions: applied potentials, −800 mV for 55 ms and then scanned to 200 mV at 20 V/s; analyte concentration, 50 μmol/l; 10 cm hydrodynamic injection for 10 s; other conditions as in Fig. 1.

3.1.2. Analyte CV studies

As described in Section 1, deformed peaks, negative peaks and irreproducible response were sometimes observed in our previous PAD studies [13]. This behavior depended on the analytes present in a mixture and on the analytes injected previously. To help understand the factors affecting electrode response of different analytes, on-line cyclic voltammograms were obtained under a variety of experimental conditions for Tl^+, Co^{2+}, Ni^{2+}, Zn^{2+}, Cd^{2+}, Cu^{2+} and Ag^+. The cyclic voltammograms of all analytes were examined with and without background subtraction to differentiate between direct electrochemical reaction of the analytes and changes in background current (faradaic or capacitance). With an Au electrode the metal ions Tl^+, Co^{2+}, Ni^{2+}, Zn^{2+} and Cd^{2+} gave normal cyclic voltammograms with no appreciable change in background current. Cyclic voltammograms of the analytes showed that the differences between the cathodic and anodic peak potentials were: 0 to 50 mV for Tl, Pb; ~200 mV for Zn; and ≥500 mV for Cd, Ni and Co. These differences in peak potentials and the cyclic voltammograms' peak shapes implied that the reversibility of the electrochemical reactions were in the following order (from fastest to slowest): $Tl^+ > Pb^{2+} \gg Zn^{2+} > Cd^{2+} \gg Ni^{2+}$ and Co^{2+}. In the cyclic voltammograms of Cu^{2+} and Ag^+, two peaks were observed. These peaks seemed to represent two different electron transfer processes, but it was also observed that the current collected in the presence of Cu^{2+} and Ag^+ was smaller than the current collected in their absence. Thus, for Cu^{2+} and Ag^+, changes in background current may have important effects on the observed cyclic voltammograms; reasons for this behavior are discussed below. The cyclic voltammograms of metal ions were also examined in 8 mmol/l succinic acid and 30 mmol/l creatinine. Similar peak shapes (relative to HIBA electrolyte) with slight shifts in peak potentials, were obtained. These shifts were likely due to differences in stability constants, and/or differences in the adsorption of anions at the electrode. The cyclic voltammograms of analytes at Pt electrodes were similar to those obtained with Au electrodes in both HIBA and succinic acid electrolytes.

To examine the effect of repeated analyte injection on the electrode response, cyclic voltammograms were recorded over repeated CE separations (up to five times). For single analytes and for mixtures, no change in behavior was observed for Tl^+, Co^{2+}, Ni^{2+}, Zn^{2+} and Cd^{2+}. However, the behavior of Pb^{2+} was different. Although repeated injection of Pb^{2+} did not affect the background cyclic voltammograms, it did change the cyclic voltammograms of Pb^{2+} and some other analytes. For example, the cyclic voltammograms of Cd^{2+} before and after repeated sampling with Pb^{2+} are shown in Fig. 3A and Fig. 3B, respectively. Fig. 3B shows that a new peak occurred at ~100 mV and that the peak potentials were shifted considerably. Some other metal ions also showed changes in their cyclic voltammograms. These results suggest that the Au surface has been changed by Pb^{2+}. Cu^{2+} and Ag^+ showed even stronger effects on Au electrode response. Noise increased following the detection of these metal ions, and a decrease in background current could be observed after Cu^{2+} or Ag^+ migrated past the Au electrode. Because the background current came mainly from the adsorption of electrolytes and charging currents, the decrease of background current suggests that the organic adsorption might have been inhibited. Results reported for scanning tunneling microscopy studies [35] have suggested that deposition of Cu^{2+} at Au and Pt surfaces can induced changes in the electrode surface. The cyclic volatmmograms of Cu^{2+} were also

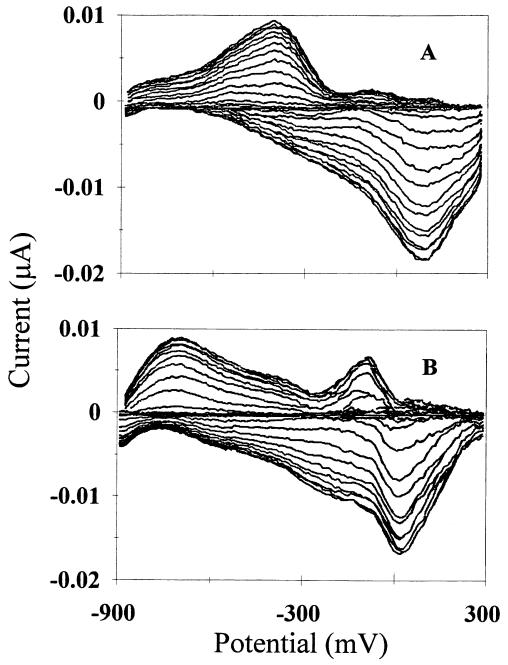

Fig. 3. Effect of injection of Pb^{2+} samples on subsequent cyclic voltammograms across Cd^{2+} peaks at 25 μm Au electrode. Experimental conditions: applied potentials, −900 mV for 55 ms and then scanned to 300 mV at 20 V/s; analyte concentration, 50 μmol/l; electromigration injection at 5.0 kV for 10 s; other conditions as in Fig. 1. (A) before injection of Pb^{2+}; (B) after the electrode was used to detect five Pb^{2+} samples.

examined in phosphoric and nitric acids, and both gave normal cyclic voltammogram peaks. These results further confirm that the decrease of background current was caused by the inhibition of organic adsorption. Similar results were also observed at Pt electrodes. The change of background current led to small or even negative signals for Cu^{2+} and Ag^{+}, and this explains the negative peaks sometimes observed for these metal ions with PAD. The nature of the changes in the Au and Pt surfaces induced by the electrochemical reactions of Pb^{2+}, Cu^{2+} and Ag^{+} is not known for certain. Incomplete removal of the analyte is a possibility, and substantial roughening of the electrode surface has been found by atomic force microscopy studies [36] for repeated deposition and stripping; such roughening is expected to change the cyclic voltammograms of analytes. To reduce these effects for Pb^{2+}, the use of a higher CV potential (400 mV) was effective, but for Cu^{2+} and Ag^{+}, the best improvements were observed with a phosphate and a nitrate electrolyte.

For Ni^{2+} and Co^{2+}, which did not show any evidence for changes in the electrode surface in the above studies, peak shape changes and baseline shifts after the peaks migrated were still observed under certain conditions. A factor in this behavior may be a change in the electrode response for H^{+} evolution. In principle, the rates of H^{+} evolution depend on the activation energy of the H^{+} reaction on the electrode surface [37], which is a function of the electrode material and its structure. In general, hydrogen has a high overvoltage on Hg, Pb, Tl, Cd and Zn surfaces; but on Fe, Ni, Co and Pt surfaces, a low overvoltage [38]. For the pH of the electrolytes (4.8), H^{+} evolution occurs at a potential ≤ -1000 mV. For Tl^{+}, Pb^{2+}, Cd^{2+}, Cu^{2+} and Ag^{+} detection the potential could be adjusted to avoid H^{+} evolution, but for Zn^{2+}, Ni^{2+} and Co^{2+} a potential of ≤ -1000 mV is needed. The H^{+} evolution observed in the cyclic voltammograms showed a decrease for Zn^{2+}, and an increase for Ni^{2+} and Co^{2+}. These changes are consistent with the H^{+} overvoltage properties of the metals. Therefore, metal ion peaks can contain responses both from the reactions of metal ions and H^{+}. In addition, small changes in the electrode surface could alter H^{+} evolution, and thus result in baseline shifts. These problems can be avoided if detection occurs during the anodic portion of a PAD pulse, which is not a limitation because this mode of data analysis usually gives maximum S/N.

3.2. Waveform shape and signal enhancement

Previous PAD studies with a simple bipolar waveform gave detection limits in the range of $2 \cdot 10^{-5}$ to $2 \cdot 10^{-7}$ mol/l [13] (note that comparisons of techniques described later are made relative to these PAD detection limits). The use of a multistep waveform should offer improved S/N for two main reasons. Firstly, multistep waveforms will permit the separation of the measurement voltage from large voltages that may be required for electrode cleaning and/or for rapid sample deposition. Secondly, the use of fast (relative to rates of diffusion) multiple-steps during signal measurement may enhance S/N due to multiple adsorption–desorptions of the ana-

lyte. In an effort to improve and widen the application of PAD, different parameters of the pulse waveform were examined over the concentration range of $1 \cdot 10^{-6}$ to $5 \cdot 10^{-5}$ mol/l; these parameters included waveform shape, waveform frequency and data collection within the pulse waveform.

According to the Cottrell equation [39], analyte and background signals observed upon the application of a voltage pulse are related to pulse frequency, and the signal/environmental noise should also increase with frequency; thus certain frequencies may give larger S/N. In previous studies with a simple bipolar pulse [13], frequencies from 4 to 8 Hz were used, and in this work signals were evaluated over the frequency range of 7.5 Hz to 600 Hz for Tl^+, Zn^{2+}, Cd^{2+} and Pb^{2+}. Square-wave pulses were applied to the electrode, and the total current was measured. The results in Fig. 4 show that for Tl^+ the analytical signal increased with pulse frequency, that peak-to-peak noise was at a minimum at 200 Hz, and that maximum S/N occurred at 180–280 Hz. The general trends observed for the other metal ions were similar to those for Tl^+. The conditions for maximum S/N (180~280 Hz) gave a three-fold enhancement in detection limits compared to those obtained previously for anodic PAD [13].

The shape of a typical multiple-step waveform used is shown in Fig. 5. A wide variety of conditions were examined over the concentration range of $1 \cdot 10^{-6}$ to $2 \cdot 10^{-5}$ mol/l, but in general the preconcentration period (t_p) was at −800 to −1200 mV for 100 to 200 ms, and signal measurement was made during the fast bipolar pulses applied with frequencies of 20 to 200 Hz over a period 100 to 200 ms; the cleaning period was at 400 to 500 mV for ~100 ms. The analytical signal used for the evaluation of different waveform shapes was the average current measured over the high-frequency pulses. The results showed that signals increased quickly for values of t_p up to 100 ms for all analytes; the rate of increase slowed down at $t_p > 100$ ms. Deposition times >200 ms decreased reproducibility of electrode response (repetitive injection R.S.D.>5%). For Pb^{2+}, which adsorbed strongly on the electrode, a high cleaning potential improved peak shape and S/N; peak width was reduced more than 50% and S/N improved up to 2- to 3-fold when a cleaning potential of 400 mV was applied for 100 ms. The application of voltage oscillations during data collection (center portion of Fig. 5) improved S/N by effectively trapping the analyte via repeated oxidation–reduction. Over the

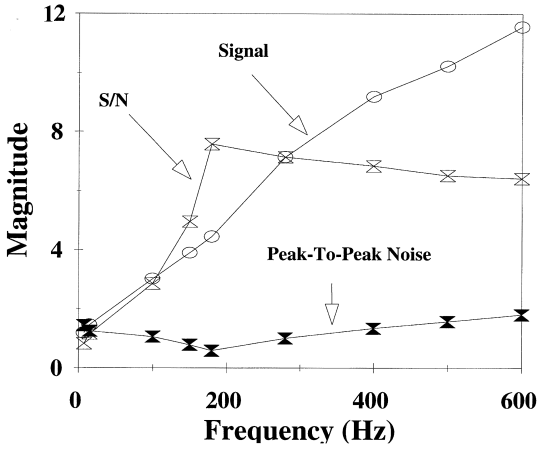

Fig. 4. Effect of bipolar pulse frequency on analytical and background signals. y-Scale is μA for signal, 0.1 μA for noise and S/N values have been divided by 10. Experimental conditions: cathodic current is considered as positive current; applied potentials, −800 mV for reduction and 200 mV for oxidation; analytical signal was an average current measured over the cathodic and anodic current; errors, ±7%; analyte (Tl^+) concentration, 2.0 μmol/l; 5 kV electrokinetic injection for 10 s; other conditions as in Fig. 1.

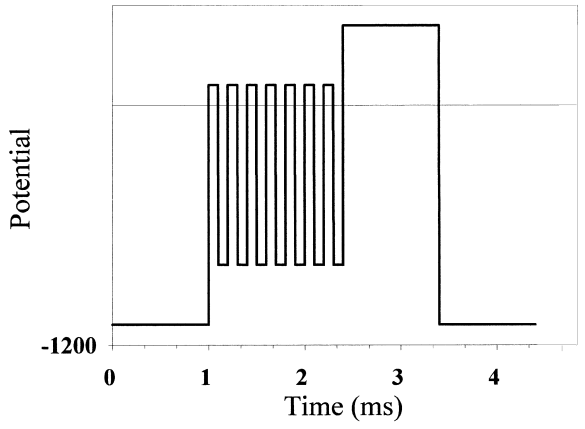

Fig. 5. Multiple-step waveform applied to electrodes. Experimental conditions: y-scale voltages depended on experiment; initial preconcentration periods were at −800 to −1200 mV (depending on analytes) for 100 to 200 ms; signal measurement was made during application of the fast bipolar pulses with frequencies of 20 to 200 Hz over a period 100 to 200 ms; the cleaning period was at 400 to 500 mV for ~100 ms.

frequency range studied (20–200 Hz) the S/N increased slowly to give a ~3-fold improvement in the range of 50–500 Hz. Above 200 Hz, background noise increased faster than analyte signals. Relative to previous results (see start of this section) obtained with a simple bipolar pulse, detection limits ($2\cdot10^{-8}$ to $2\cdot10^{-7}$ mol/l) were improved by up to 10-fold for Tl^{+} and Pb^{2+}, and by 4–6 fold for the other metal ions studied. Cleaning periods of ~100 ms in the waveform were sufficient to prevent longer-term accumulation of the analytes, which would cause peak broadening. The maximum pulse length was limited to 400 ms to permit the collection of 10 data points for a 4 s peak.

Since the ratio of background and faradaic currents also depends on the location of data sampling within a pulse, optimizing of the data collection period may provide larger S/N. To find the sampling location having maximum S/N, a 180 Hz frequency bipolar pulse was sampled over 64 equal sampling periods for Tl^{+}, Zn^{2+}, Cd^{2+} and Pb^{2+}: each period was ~0.087 ms. All analytes exhibits similar trends, and the response for Tl^{+} and Cd^{2+} across one square-wave pulse at the maximum of the CE peaks are shown in Fig. 6. For both anodic and cathodic signals, maximum response was obtained at ~0.2 ms after the change of potential polarity. Although peak-to-peak noise was also a maximum at the same point, S/N was still a maximum at 0.2 ms. Theoretically, maximum electrode response should immediately follow the change of potential polarity, and the small delay observed in Fig. 6 may be a result of delays in the data acquisition board; such shifts have been reported elsewhere [40]. When the optimal sampling period (~0.2) ms was used for CE separation of the test metal ions over the concentration range of $5.0\cdot10^{-6}$ to $1.0\cdot10^{-4}$ mol/l it was found that the anodic signal gave slightly better detection limits (by ~2:1). However, these detection limits were poorer than those observed previously for integration of the whole anodic signal, and thus this was not investigated further.

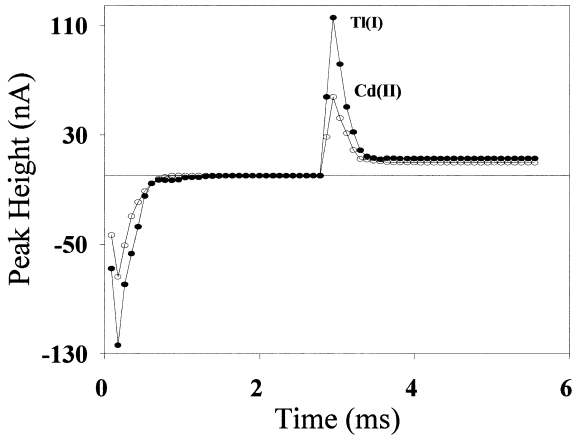

Fig. 6. Response for Tl^{+} and Cd^{2+} at different points of applied bipolar pulse. Experimental conditions: applied bipolar pulse potentials, −1000 mV for reduction and 300 mV for oxidation with a frequency of 180 Hz; analytical data were collected over each short period (0.087 ms); errors, ±6%; analyte concentration, 20 μmol/l; other conditions as in Fig. 4.

3.3. Signal analysis techniques

3.3.1. Harmonic analysis

As discussed above, Fourier analysis of PAD currents might offer a technique to differentiate between the symmetrical double-layer capacitance currents and the less symmetrical faradaic currents. To determine if this approach might improve S/N the magnitudes of the different harmonics were examined for the CE separation of Tl^{+}, Cd^{2+}, Pb^{2+}, Zn^{2+}, Ni^{2+} and Co^{2+}, over the concentration range of $1\cdot10^{-4}$ to $5\cdot10^{-6}$ mol/l with a PAD frequency range of 7.5 to 120 Hz. A typical response observed for a CE separation with normal PAD obtained by application of a 75 Hz square-wave pulse is shown in Fig. 7. The CE data in this Figure has been displayed as both the average current (curve A) and as the total current (curve B, cathodic–anodic). Both curves in Fig. 7 exhibit a shifted baseline, a feature often observed for these analytes when cathodic currents contribute to the signal used for analysis (see Section 3.1). The average-current response is expected to be smaller for symmetrical signals (fast, reversible reactions), and this is one of the reasons for the difference in relative peak heights between curves A and B in Fig. 7. The S/N for the peaks in curve B are similar to previous results for anodic detection [13], but baseline stability was much poorer because cathodic currents were part of the analytical response. The S/N values in curve B were used as a standard for comparison of the different signal-perceiving techniques discussed below. Curve A in Fig.

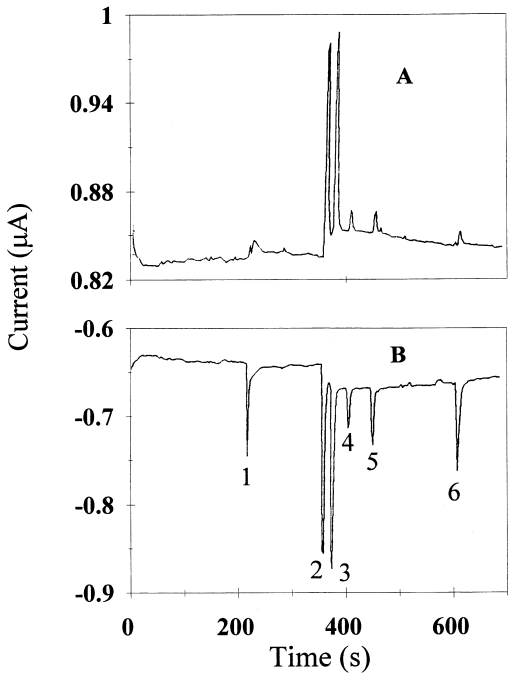

Fig. 7. Electropherogram of metal ions with bipolar pulsed amperometric detection. Experimental conditions: cathodic current is considered as positive current; applied potentials, −700 mV for reduction and 300 mV for oxidation with a frequency of 75 Hz; analyte concentration, 50 μmol/l; curves A and B represent average and total currents, respectively; peak identification, 1= Tl^{+}; 2=Co^{2+}; 3=Ni^{2+}; 4=Zn^{2+}; 5=Cd^{2+}; 6=Pb^{2+}; other conditions as for Fig. 4.

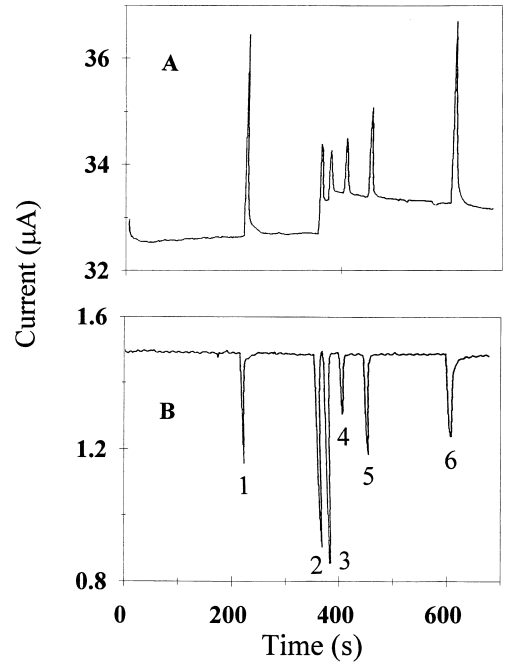

Fig. 8. Electropherograms obtained using first (curve A) and second (curve B) harmonics. Experimental conditions: fundamental frequency is 75 Hz; data used for the analysis are those that collected in Fig. 7; peak identification and other conditions as in Fig. 7.

8 shows the electropherogram obtained at the fundamental frequency. Since this frequency is expected to contain the major portion of all symmetrical signals, it is not surprising to find that peaks for the more irreversible analytes, Co^{2+} and Ni^{2+} (peaks 2 and 3) are reduced (relative to other peaks) compared to normal PAD (total current, curve B, Fig. 7). It can also be seen that Zn^{2+} and Cd^{2+}, which have an intermediate reversibility, follow slightly different patterns relative to the other metal ions. When the second harmonic is used for the electropherogram (curve B, Fig. 8) unsymmetrical signals are detected. Thus relative peak heights for Co^{2+} and Ni^{2+} are increased, and are similar to that observed for the total current in curve B of Fig. 7. Two other important features to note for the response for the second harmonic are the lower overall signal strength and the more stable baseline; both of these features are likely a result of the removal of symmetrical components. In spite of the lower signal in curve B of Fig. 8, there is still an enhancement of S/N by 2- to 4-times relative to curve B of Fig. 7. An evaluation of this approach over a wide range of conditions gave improvements in S/N that were essentially the same. The detection limits for Ni^{2+} and Co^{2+} were ~3-fold improved relative to PAD, and for other metal ions, detection limits were similar.

In some cases the use of a lock-in amplifier can offer improved S/N as a method for the isolation of harmonics. Consequently this approach was examined over the frequency range of 7.5 to 1000 Hz for square-wave pulses, and the applied frequency was used as the reference frequency of the lock-in amplifier. The results showed little (maximum 3-fold) or no improvement in S/N relative to previous anodic detection [13] for either the first or second harmonic. Such a small improvement may be because the optimal frequency for a lock-in amplifier is from a few hundred Hz to 10 kHz. At low fre-

quencies, $1/f$ noise, including both that developed in the Model 5301 lock-in amplifier and that originating in the experiment itself, may have limited the S/N of the lock-in amplifier for low-frequency signals. At high frequencies, the lock-in amplifier could not differentiate the analytical signal from the background noise.

3.3.2. Phase sensitive detection

An alternative approach for minimizing contributions from capacitance currents is to treat the currents as vectors and to use a phase angle shift to minimize contributions from charging currents (see Section 2.4). The results for this approach with the first and second harmonics are shown in Fig. 9. Again, the best improvements in S/N were seen for Co^{2+} and Ni^{2+}, and in general the trends are similar to those shown in Fig. 8. Thus the second harmonic response, curve B in Fig. 9, showed improved baseline stability and better S/N. The improvements in S/N were 3- to 6-fold relative to total current (curve B, Fig. 7), and thus this approach is slightly better than that for the harmonic analysis conditions used in Fig. 8.

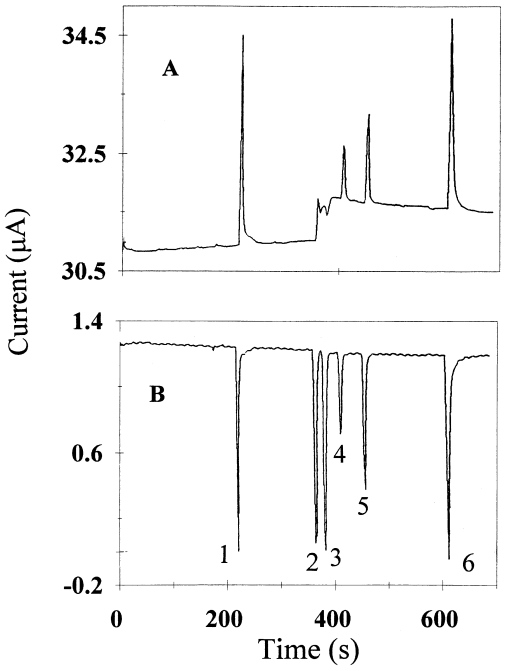

Fig. 9. Electropherograms obtained using first (curve A) and second (curve B) harmonics from vector analysis. Experimental conditions as in Fig. 7.

4. Conclusions

Of the various approaches examined for the enhancement of analytical S/N, the best results were obtained with the addition of a multiple-step potential waveform to a bipolar pulse. The up to 10-fold improvements (detection limits in $2\cdot10^{-8}$ to $2\cdot10^{-7}$ mol/l range) observed relative to PAD are mainly applicable to species that can be concentrated at the electrode, but such approaches may also prove useful for analytes that physically adsorb at electrode surfaces. Although the harmonic analysis techniques offered improved baseline stability, the smaller improvements in S/N (3- to 6-fold for vector approach) make this approach a bit less attractive. However, this procedure may prove useful for application to analytes that cannot be preconcentrated at the electrode surface. Digital filtering and data smoothing techniques can also be used to further improve S/N. A brief examination of these techniques showed improvements of 2–5-fold, but a controlled study was not made for all the different approaches examined for PAD in this paper. Another detection approach, which has not been examined in these studies, is the use of rapid-scanning CV. From the preliminary work done here to characterize electrode–analyte interactions it is apparent that this type of CE detection may combine sensitive detection with analyte characterization. This aspect will be the subject of a future investigation.

Acknowledgements

The authors acknowledge the Natural Science and Engineering Research Council of Canada and the Waters Corp. for financial assistance to certain portion of this research.

References

[1] R.A. Wallingford, A.G. Ewing, Anal. Chem. 59 (1987) 1762.
[2] C.D. Gaitonde, P.V. Pathak, J. Chromatogr. 514 (1990) 389.

[3] D.S. Austin, J.A. Polta, J. Electroanal. Chem. 168 (1984) 227.
[4] S.E. Moring, in: P.D. Grossman, J.C. Colburn (Eds.), Capillary Electrophoresis – Theory and Practice; Quantitative Aspects of Capillary Electrophoresis Analysis, Academic Press, San Diego, CA, 1992.
[5] D. Clark, M. Fleishman, D. Pletcher, J. Electroanal. Chem. 37 (1972) 137.
[6] A. MacDonald, P.D. Duke, J. Chromatogr. 83 (1973) 331.
[7] J.A. Polta, D.C. Johnson, J. Liq. Chromatogr. 6 (1983) 1726.
[8] L.E. Welch, W.R. LaCourse, D.A. Mead Jr., T. Hu, D.C. Johnson, Anal. Chem. 61 (1989) 555.
[9] S. Hughes, D.C. Johnson, Anal. Chim. Acta 149 (1983) 1.
[10] W.R. LaCourse, D.A. Mead Jr., D.C. Johnson, Anal. Chem. 62 (1990) 220.
[11] J.A.M. vanRiel, C. Olieman, Anal. Chem. 67 (1995) 3911.
[12] A. Ngoviwatchai, D.C. Johnson, Anal. Chim. Acta 215 (1988) 1.
[13] J. Wen, R.M. Cassidy, Anal. Chem. 68 (1996) 1047.
[14] I. Morita, J. Sawada, J. Chromatogr. 641 (1993) 375.
[15] F.M. Everaerts, T.P.E.M. Verheggen, F.E.P. Mikkers, J. Chromatogr. 169 (1992) 341.
[16] R.L. Chien, D.S. Burgi, Anal. Chem. 64 (1992) 1046.
[17] A. Hussam, Anal. Chem. 60 (1988) 2776.
[18] C.W.K. Chow, D.E. Davey, D.E. Mulcahy, T.C.W. Yeow, Anal. Chim. Acta 307 (1995) 15.
[19] P.W. Alexander, J. Koopetngram, Anal. Chim. Acta 197 (1987) 353.
[20] W. Matuszewski, A. Hulanicki, M. Trojanowicz, Anal. Chim. Acta 194 (1987) 269.
[21] T.J. O'Shea, S.M. Lunte, Anal. Chem. 65 (1993) 948.
[22] A.J. Bard, L.R. Faulkner, Electrochemical Methods – Fundamental and Applications, Wiley, New York, 1980, Ch. 9.
[23] P. Singhal, W.G. Kuhr, Anal. Chem. 69 (1997) 3552.
[24] J.G. White, J.W. Jorgenson, Anal. Chem. 58 (1986) 2992.
[25] S.S. Ferris, G. Lou, A.G. Ewing, J. Microcol. Sep. 6 (1994) 263.
[26] S. Park, M.J. McGrath, M.R. Smyth, D. Diamond, C.E. Lunte, Anal. Chem. 69 (1997) 2994.
[27] P. Jandik, G. Bonn, Capillary Electrophoresis of Small Molecules and Ions, VCH, New York, 1993, Ch. 3.
[28] W. Lu, R.M. Cassidy, A.S. Baranski, J. Chromatogr. 640 (1993) 433.
[29] P. Avouris, J.E. Demoth, J. Chem. Phys. 75 (1981) 4783.
[30] L. Stolberg, J. Lipkowski, D.E. Irish, J. Electroanal. Chem. 296 (1990) 271.
[31] A. Hamelin, J. Electroanal. Chem. 138 (1982) 395.
[32] A.J. Bard, L.R. Faulkner, Electrochemical Methods – Fundamental and Applications, Wiley, New York, 1980, Ch. 12.
[33] C.-H. Chen, S.M. Vesecky, A.A. Gewirth, J. Am. Chem. Soc. 114 (1992) 451.
[34] D.J. Trevor, C.E.D. Chidsey, D.N. Loiacona, Phys. Rev. Lett. 62 (1989) 929.
[35] A. Bewick, B. Thomas, J. Electroanal. Chem. 84 (1977) 127.
[36] V. Jovic, B. Jovic, A. Despic, J. Electroanal. Chem. 288 (1990) 229.
[37] R. Parsons, Trans. Faraday Soc. 54 (1958) 1035.
[38] H. Gerischer, Trans. Faraday Soc. 67 (1958) 506.
[39] D.K. Gosser, Cyclic Voltammetry – Simulation and Analysis of Reaction Mechanisms, VCH, New York, 1993.
[40] W. Lu, R.M. Cassidy, Anal. Chem. 63 (1993) 2878.